

## DNA fragmentation by gamma radiation and electron beams using atomic force microscopy

Luis Nieto González · João D. T. Arruda-Neto · Monica A. Cotta ·  
Helaine Carrer · Fermin Garcia · Ricardo A. S. Silva ·  
Antonio L. D. Moreau · Henriette Righi · Godofredo C. Genofre

Received: 4 October 2011 / Accepted: 24 April 2012 /  
Published online: 27 May 2012  
© Springer Science+Business Media B.V. 2012

**Abstract** Double-stranded pBS plasmid DNA was irradiated with gamma rays at doses ranging from 1 to 12 kGy and electron beams from 1 to 10 kGy. Fragment-size distributions were determined by direct visualization, using atomic force microscopy with nanometer-resolution operating in non-tapping mode, combined with an improved methodology. The fragment distributions from irradiation with gamma rays revealed discrete-like patterns at all doses, suggesting that these patterns are modulated by the base pair composition of the plasmid. Irradiation with electron beams, at very high dose rates, generated continuous distributions of highly shattered DNA fragments, similar to results at much lower dose

---

L. Nieto González · F. Garcia  
Departamento de Ciência e Tecnologia, Universidade Estadual de Santa Cruz, Ilhéus, BA, Brazil

J. D. T. Arruda-Neto (✉) · R. A. S. Silva · H. Righi  
Instituto de Física, Cidade Universitária Armando de Salles Oliveira,  
Universidade de São Paulo, São Paulo, SP, Brazil  
e-mail: arruda@if.usp.br

J. D. T. Arruda-Neto · G. C. Genofre  
CEPESq/Unifitalo – Italy-Brazilian University Center, São Paulo, SP, Brazil

M. A. Cotta · A. L. D. Moreau  
Instituto de Física, Cidade Universitária Zeferino Vaz,  
Universidade Estadual de Campinas, Campinas, SP, Brazil

H. Carrer  
Escola Superior de Agricultura Luiz de Queiroz, Departamento de Ciências Biológicas,  
Universidade de São Paulo, Piracicaba, SP, Brazil

G. C. Genofre  
Biosciences Institute, University of São Paulo, São Paulo, SP, Brazil

rates found in the literature. Altogether, these results indicate that AFM could supplement traditional methods for high-resolution measurements of radiation damage to DNA, while providing new and relevant information.

**Keywords** Plasmid DNA · Fragment-size distributions · AFM · Gamma radiation · Electron beams

## 1 Introduction

Size and distribution analysis of breaks in DNA is one of the most important and up-to-date methods for the study of this molecule. Mostly used techniques are based on gel electrophoresis or elution of DNA [1–4]. To a greater or lesser extent, these are limited techniques because of their inability to resolve individual DNA fragments (less than 10 kbp [5]). As a consequence, interpretation of results requires complex theoretical models and only average quantities can be determined. It is thus implied by this shortcoming that DNA breaks occur at random, a general assumption inherent in models of DNA radiation damage used over the last two decades [6–9]. However, experiments have shown that the distribution profiles of DNA fragments differ significantly from random DSB model predictions [10, 11]. For example, a higher proportion of small fragments from DNA irradiated with heavy ions has been reported by Rydberg [12]. This makes clear the necessity for a technique not based on a random model for data interpretation, and at the same time, able to resolve the spatial distribution of shorter fragments. In other words, a more direct method would allow the counting and measurement of individual DNA fragments.

The advent of atomic force microscopy (AFM) in 1986 introduced the possibility of directly visualizing biological molecules with molecular or atomic resolution, even in the molecule's physiological environment [13]. DNA molecules have been imaged and studied extensively with this technique both in air and in aqueous solutions [14–16]. AFM technology has been applied in the tapping mode for image-based investigation of biochemical processes such as KU and ATM proteins binding to DNA [17, 18]. Investigation of radiation-induced DNA damage with this technique has provided results comparable to those from gel electrophoresis [18, 19].

Pang and collaborators successfully used AFM to study radiation damage in plasmid DNA, aiming at determining a relationship between the number of double-strand breaks (DSB) versus radiation dose, and size evaluation of fragments. Basically, pCU19 plasmids in aqueous solution were irradiated with electrons (6.0 MeV) and neutrons (0.71 MeV) at different doses [20–23]. It was observed that the number of small fragments (restricted to the 10–50 nm length interval) increases with dose, following an exponentially decreasing relationship such that at high doses (approximately 10 kGy and 8 kGy for neutrons and electrons, respectively) the plasmids were totally shattered into smaller fragments, indicating the occurrence of multiple consecutive breaks. Enhanced production of DNA small fragments by electrons has also been reported elsewhere [10, 24] using AFM.

Here, DNA fragmentation induced by irradiation with gamma rays and electrons is studied. Of these, the gamma ray is a more subtle irradiation probe, implying that fine structural aspects of the strands are better preserved vis-à-vis neutrons and heavy ions. A new and finer methodology for preparation of plasmids (linearization, dephosphorylation, etc.) is also developed and used here, while many factors negatively affecting AFM image resolution (temperature, tip probe, measurement mode, humidity, etc.) are circumvented.

All this allows for assessment of fragment spatial distributions with length resolution around 10–15 nm (30–45 bp, approximately).

## 2 Materials and methods

### 2.1 DNA samples – preparation and irradiation

Double-stranded pBS plasmid DNA was used, prepared at a concentration of 1000 ng/ml in TE buffer. This plasmid is approximately 2900 bp (~940 nm) long (assuming 3.4 nm per 10.5 bp for B-type DNA [25]), with a width of 1.9 nm. For irradiation and AFM imaging, the naked DNA plasmid was diluted at 5 ng/ml in 10 mM Hepes and then divided into aliquots in 0.5-ml plastic microcentrifuge tubes, each containing 100 ml of the DNA solution. No additional free-radical scavenger was added to the Hepes buffer. The extraction and purification of DNA were done using the “Invisorb Plasmid Kit”, according to the manufacturer’s specifications. Linearization was performed with the enzyme HindIII, also following the manufacturer’s specifications. Finally, in order to prevent rejoining, the linearized DNA was dephosphorylated with the aid of the enzyme Calf Intestine Alkaline Phosphatase (CIAP). All samples were exposed to air during their handling.

DNA samples were irradiated with electron beams and gamma rays at doses ranging from 1 to 10 kGy and from 1 to 12 kGy, respectively. All irradiations were performed at the facilities of the Institute for Energy and Nuclear Research in São Paulo (IPEN).

Electron beams were delivered by a linear electron accelerator (Dynamitron, model JJOB 188, RDI Radiation Dynamics, Inc.) operating with an energy of 1.174 MeV and average beam intensity of 0.5 mA. The samples were accommodated in a conveyor belt loop, exposing the samples to electron beams at intervals of 3 min (conveyor belt lap time). Each exposure imparting a dose of 0.5 kGy lasted only 0.223 s, which corresponds to an instantaneous dose rate of  $8 \times 10^3$  kGy/h, approximately. The average dose rate was 10 kGy/h.

Irradiation with gamma rays was performed at the Gamma-Cell CTR-IPEN (locally designed and constructed) operated by the Product Overlapping Source system. This facility provides 1.25 MeV gammas from Co-60 at a dose rate of 2.4 kGy/h. Each irradiation was assisted by a control sample.

### 2.2 DNA imaging with AFM – distributions of fragment length

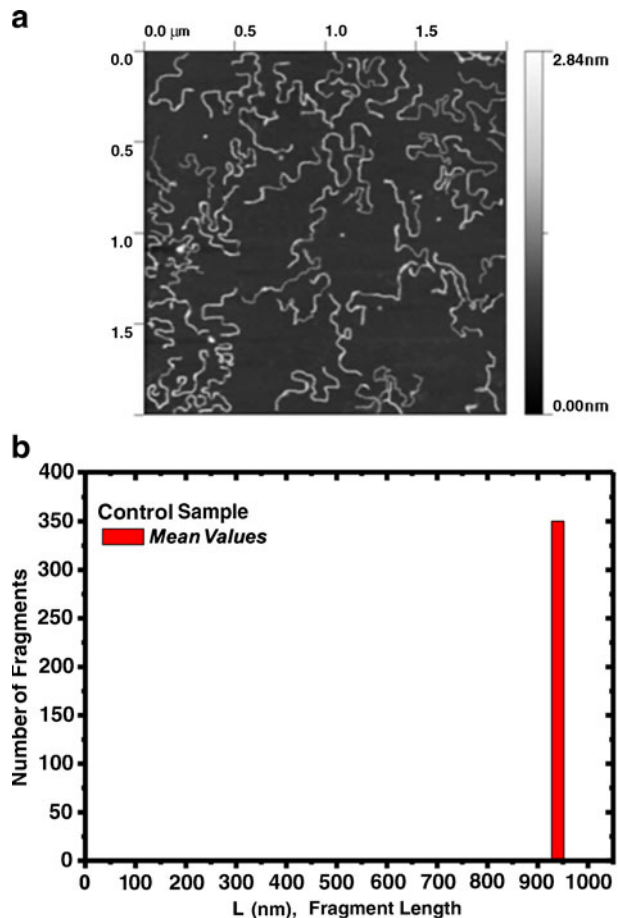
Several modes of operation can be used, depending on the type of surface (material) and even microscope type. The microscopes used in this study are the AutoProbe CP (ThermoMicroscopes) and the Agilent-5500. For DNA imaging, the AFM was operated in air and non-tapping mode. Conical silicon tips were used with typical curvature radius of 10 nm and aspect ratio of 3:1, mounted on cantilevers with resonance frequency around 80 kHz and spring constant in the range of 1.8 to 3.2 N/m. Sample preparation for AFM imaging consisted of the deposition of 1 ml of aqueous DNA solution on an atomically flat mica surface, followed by a gentle rinse using a few drops of distilled water. 1 mM MgCl<sub>2</sub> was deposited on the mica substrate to assure the adhesion of DNA molecules. Before placing the DNA sample on the mica foil, MgCl<sub>2</sub> excess was removed by washing with distilled water. The DNA sample on the mica was then dried in a gentle flow of nitrogen gas for 5 min and DNA fragment-length measurements were performed with the Agilent-

5500 software, allowing segmented measurements of a curved fragment. The length of each segment was measured and accumulated to yield the length of the entire curved fragment. The resolution of the AFM in these measurements (usually quite low) was estimated from the *finer structure* of size distributions since, as shown in Section 3, these distributions exhibit normal Gaussian-like statistic characteristics.

The distribution of fragment lengths is based on assigning the measured length of each fragment to the closest 50-nm-wide bin in the range of 0 to 1,000 nm. For example, the bin designated by its upper end of 150 nm has all fragments between 101 and 150 nm and has a centroid equal to 125 nm. The fragment-length data were plotted as a function of the bin-range upper end of the length designation. There are roughly 150 bp in a 50-nm bin width.

Results shown in Figs. 3, 4 and 5, corresponding to different doses, are average values obtained from multiple measurements (several AFM images). Firstly, data from each image were normalized to the total number of fragments in the specific image. Next, all these normalized results from several images, and referring to a specific dose, were averaged out—this final result was used to draw the histograms.

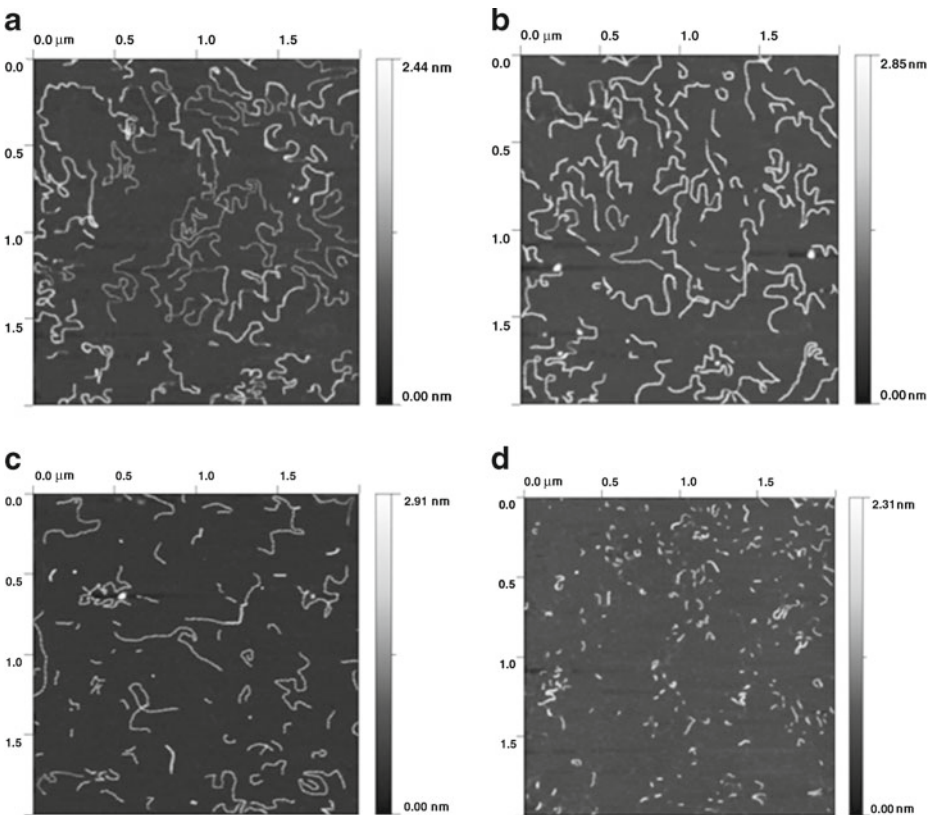
**Fig. 1** Non-irradiated pBS DNA plasmid. **(a)** AFM  $2 \times 2 \mu\text{m}$  control sample image. **(b)** Number of fragments as a function of their length



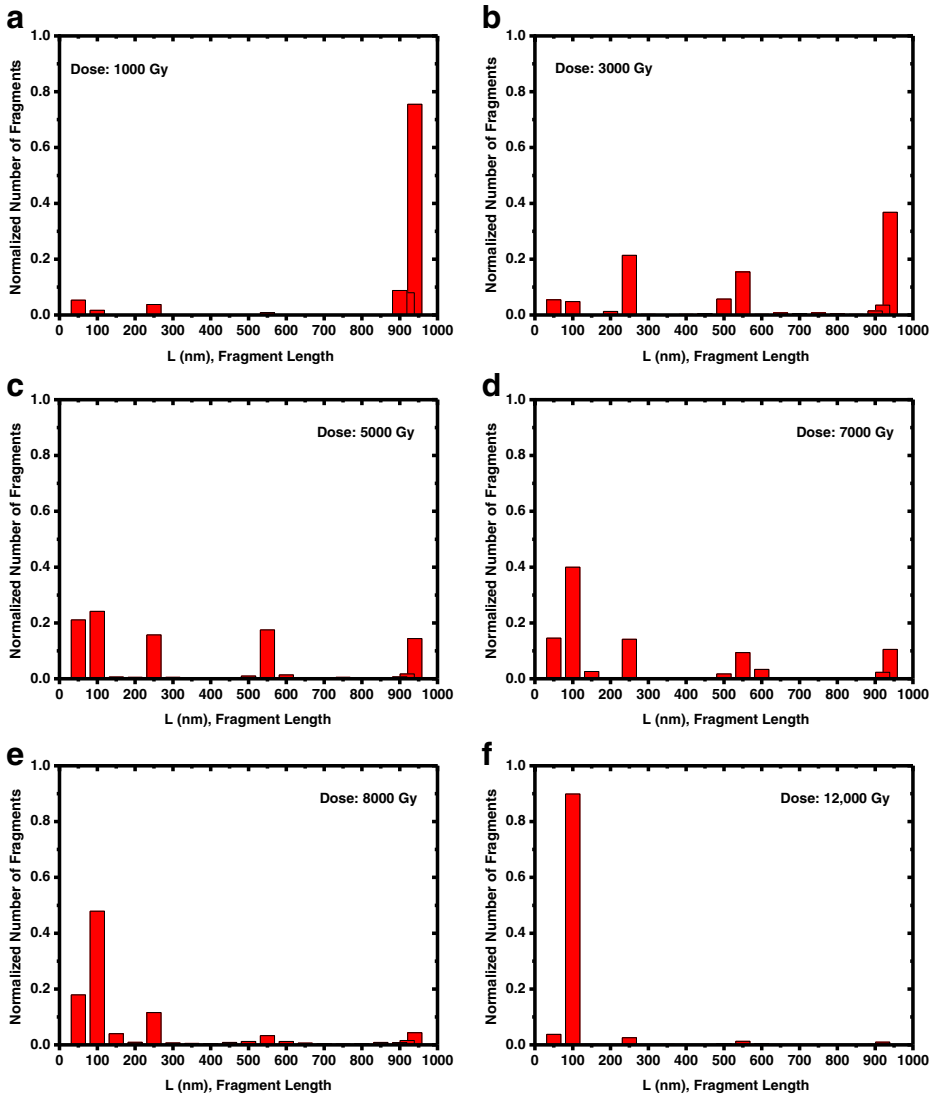
### 3 Results

Figure 1a shows an AFM image of the non-irradiated pBS plasmid DNA, allowing for verification of the plasmid lengths as well as their concentration in the image. Figure 1b shows the concentration (number of fragments) of plasmids as a function of length in the AFM image (Fig. 1a). Seven different control samples with different AFM settings and substrate surface areas were measured, and the result shown in Fig. 1b is the average of all these data. Our results show that size distributions in Fig. 1b do not change when control samples are submitted to conditions such as transport for irradiation and handling.

Seven samples of pBS DNA plasmid, all of them with the same concentration of 5 ng/ml, were irradiated with gamma rays at the same conditions with doses between 1 and 12 kGy. The AFM scanning of each sample produced about 30 images all over its extension, which considerably reduced systematic errors. Some of these 30 images per sample are shown in Fig. 2 for illustration purposes. Thus, they correspond to a small fraction of the entire scanned sample. Actually, the assessed number of plasmid fragments in each sample ranged from several hundreds to over a thousand. It should also be pointed out that plasmids irradiated at high doses are severely shattered into quite small fragments (see Fig. 3d–f). However, there must be limits to the sizes as, for instance, a *fragment minimum*



**Fig. 2** AFM  $2 \times 2 \mu\text{m}$  images sequence of irradiated pBS plasmids. (a) 1,000 Gy, (b) 3,000 Gy, (c) 5,000 Gy, and (d) 12,000 Gy

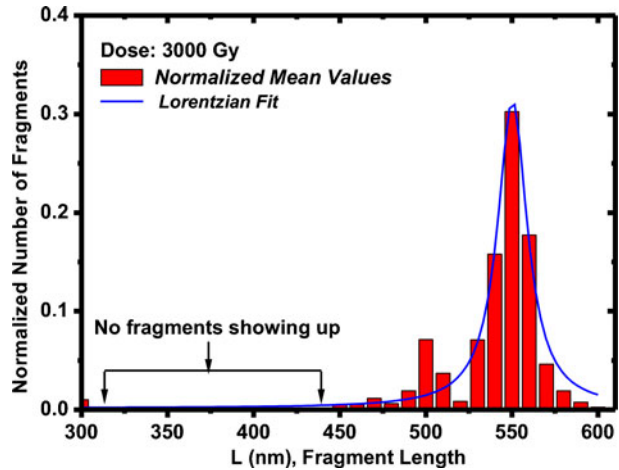


**Fig. 3** Results for gamma-irradiated pBS plasmid DNA. (a) 1,000 Gy, (b) 3,000 Gy, (c) 5,000 Gy, (d) 7,000 Gy, (e) 8,000 Gy and (f) 12,000 Gy. The *histogram bars* represent the normalized mean values

*length*. Checking of reproducibility was performed by measuring samples twice at doses of 5,000 and 8,000 Gy on different days (interval of about 30 days).

Distributions obtained at each gamma dose are shown in Fig. 3. As explained in Section 2, the distributions of fragment lengths were obtained by grouping the measured lengths into bins of 50-nm intervals. Therefore, all histograms were constructed as 50 nm wide. For example, the first histogram (labeled 50 nm) houses fragment lengths between 25 nm and 75 nm. However, a typical *finer structure* underlying all the 50-nm-wide histograms is shown in Fig. 4 by means of 10-nm-wide histograms, where the peak centered at 550 nm is constituted by fragments lengths ranging from 545 to 550 nm and from 550

**Fig. 4** Amplification of the region around 550 nm in Fig. 3b, with the fragment-length distribution at intervals down to 10-nm



to 555 nm. This most prominent peak at 550 nm was fitted by a Lorentzian curve, similar to a Gaussian except for having more pronounced tails, which is a more frequent occurrence in experimental distributions. The full width at half maximum (FWHM) of this curve is smaller than 20 nm, which is quite compatible with the scanning bin of 10 nm. This data analysis demonstrates that the *upper limit* of the achieved resolution is 10 nm (FWHM / 2).

A marked qualitative and quantitative difference of all fragment distributions as function of doses is clearly observed. Quite surprisingly, the distributions show a discrete pattern indicating that the strand breaking probability is not the same all along the plasmid length (more details below).

The results for DNA irradiated with electron beams are shown in Fig. 5. Two columns are displayed in this figure, one with the AFM images and another showing the concentration (number of fragments) of plasmids as function of their length. The distributions obtained are quite distinct at each of the doses ranging from 1 to 10 kGy.

## 4 Discussion

### 4.1 Fragmentation patterns obtained with electrons

The results obtained by irradiation with electrons (Fig. 5) are qualitatively similar to those of Pang and collaborators [23]. It is noted in our results that the number of small-size DNA fragments increases continuously and exponentially with doses greater than 3 kGy. One could be led to conjecture that very high electron dose rates could lead to finer shattering of the plasmid strands, as suggested by the results at 10 kGy where the strands were all shattered down to 50 nm sizes (Fig. 5). However, this is not the case.

The average electron dose rate in this study was 167 Gy/min (10 kGy/h), and the instantaneous dose rate  $8 \times 10^3$  kGy/h, while in all the experiments conducted by Pang et al. with electrons, it was 48 Gy/min (or, 2.9 kGy/h), quite close to the 2.4 kGy/h of the Co-60 gamma source (see Section 2). Despite the great differences in the dose rate regimes from the linear accelerators of these two laboratories, the results are highly comparable, particularly when referring to the fragmentation ability of electrons (see e.g., Fig. 3b in

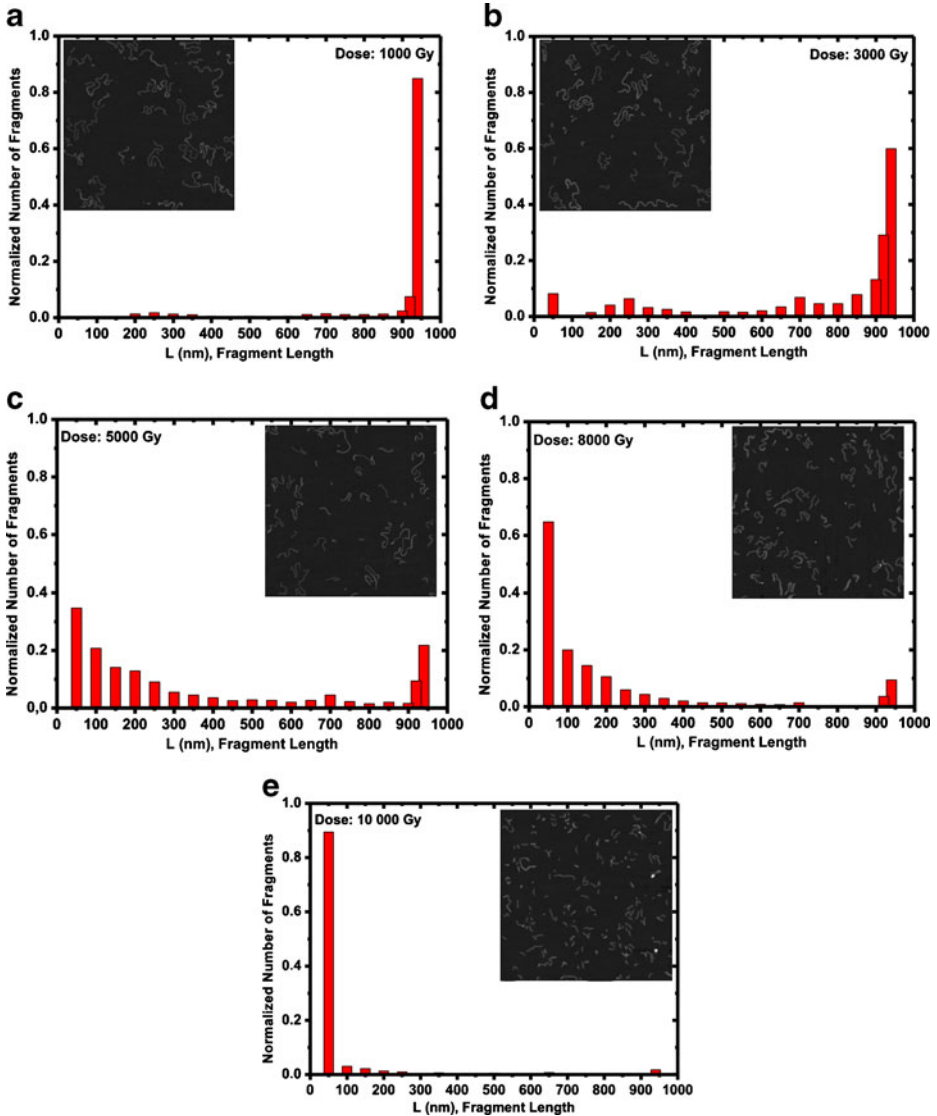


**Fig. 5** Results for irradiations of the pBS plasmid DNA with electrons. **(a)** 1,000 Gy, **(b)** 3,000 Gy, **(c)** 5,000 Gy, **(d)** 8,000 Gy and **(e)** 10,000 Gy. The *histogram bars* represent the normalized mean values

Ref. [23]). Therefore, the plasmid fragmentation patterns observed with electron beams are nearly unaffected by different dose rates, all exhibiting an exponential-like behavior. We note in this regard that (a) if the number of fragments  $N(L)$  decreases to  $N(L) - dN$ , when their lengths increase from  $L$  to  $L + dL$ , and (b) if such a variation  $dN$  is stochastic and equally probable at all intervals  $dL$ , the *relative probability distribution* of fragment sizes,  $p(L)$ , is a constant. Specifically,

$$p(L) = -(1/N) dN/dL = \lambda, \tag{1}$$



where  $\lambda$  is a function only of the dose, regardless of the mechanisms underlying the DNA breakage. The solution of (1) is

$$N = N_0 \cdot \exp(-\lambda L). \quad (2)$$

This solution is well known and quite obvious, but a more profound insight is provided by (1)—it is a *stochastic condition*. Thus, *exponential-like decaying functions*, as most of the fragment size distributions obtained with electrons in this study and elsewhere [20–23], are signatures of stochastic phenomena where all the observed events are equally probable per unit of the independent variable.

#### 4.2 Fragmentation patterns obtained with gamma rays

From our results of gamma irradiation of the pBS plasmid DNA (Fig. 3), the following aspects are noted:

1. Distributions with discrete-like pattern at all doses in the wide 1 kGy–12 kGy range, using a 50-nm-wide scanning bin.
2. The distribution structures remain nearly in the same positions for all doses, except at the extremes of the dose range (1 kGy and 12 kGy—Fig. 3), but their heights (the number of fragments) gradually increase toward smaller sizes as doses are augmented.

These two aspects of our results clearly indicate that the strand-breaking probability is not the same all along the pBS plasmid length. Unlike electrons, a fragment-size distribution generated by gamma rays is by no means stochastic. Thus, a possible and more likely conclusion is that the pBS plasmid strands are constituted by regions more favorable to breakdown when hit by gamma rays.

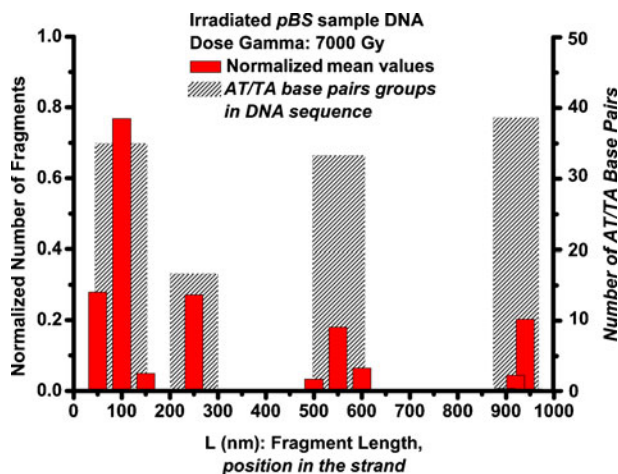
##### 4.2.1 Correlation between fragment distribution and plasmid base pair structure—an educated guess

The DNA sequence of the pBS plasmid, in terms of its AT/TA base pair composition, was quantitatively analyzed. The sequence of this plasmid is well known, and available from many Internet links [26]—it is a map of 2,900 base pairs. We merely performed a counting of AT/TA and GC/CG base pairs, sampling all the groups having more than 20 AT or TA per 100 nm strand interval.

Results are shown in Fig. 6 along with our experimental data obtained at 7,000 Gy. The horizontal scale indicates the strand position of the base pairs, corresponding at the same time to the measured fragment lengths. The remarkable overlapping of these two sets of data is quite evident. Although a definitive explanation for this finding requires further study, the two sets of results shown in Fig. 6 suggest the existence of a correlation between the pattern of fragment sizes and the pBS plasmid base pair composition. Interestingly too, such a modulation is damped in irradiations with electrons.

In fact, the most surprising difference between the results obtained with electrons and gamma rays refers to the *fragment-size distribution patterns*. On one hand, the discussion presented above indicates that dose rates play no role in this regard. The comparison shown in Fig. 6, on the other hand, suggests that the distribution pattern observed with gamma irradiation is dictated by the base pair composition of strands. Why the same did not occur with electron irradiation remains unanswered, but some possibilities are discussed in Section 4.3 below. However, a possible explanation for the fact that breaks are more likely to occur at the AT-rich portions of the strands is discussed below.

**Fig. 6** Fragment-length distribution for 7,000 Gy (*narrower bars, left-handed scale*) and the corresponding number of AT/TA bp (*shaded histograms, right-handed scale*)



#### 4.2.2 Stiffness of GC-rich regions

Actually, GC-rich regions are stiffer. DNA molecules that contain a greater proportion of GC pairs require higher temperatures to denature because the three hydrogen bonds in GC pairs make them more stable than AT pairs with two hydrogen bonds [27]. Relevant implications of higher conductivity in GC-rich DNA could be its key role in a plethora of essential properties such as, energy dissipation, molecular signaling, and eventually, DNA integrity preservation. An intriguing possibility is that guanine-rich regions of DNA serve as “cathodic” protectors. In fact, since guanine has the smallest oxidation potential compared to the other bases, long-range charge transfer of holes to short guanine-rich protuberances at the termini of chromosomes could protect DNA from oxidative stress [28].

#### 4.3 The irradiation issue

The precise mechanism by which radiation causes breaks in DNA strands is not completely established. The prevailing view is that this DNA damage is predominantly caused by the breaking of chemical bonds (and subsequent formation of free radicals) by direct impact of high-energy particles of the incident radiation on water molecules of the medium, but this has been challenged by recent evidence showing that DNA damage can also be caused by low-energy (below about 20 eV) secondary electrons that are generated by the incident radiation. The implications of this are potentially significant as secondary electrons represent the most abundant species formed along a radiation track in condensed matter (roughly  $5 \times 10^4$  secondary electrons are produced per 1 MeV *primary energy deposited*) [29–31].

Electrons are charged particles which, therefore, deposit most of their energies in the molecules of the medium (water, in general) producing a great number of secondary electrons. Thus, copious fluxes of secondary electrons equally and intensively “illuminate” the whole DNA length, and all sites would have the same breaking probability per unit length fragment. Gamma rays, on the other hand, are electromagnetic waves. As a zero-electric-charge radiation, the stopping power of gamma rays in water is smaller than electrons and, as a consequence, the production of secondary electrons is considerably reduced.

In fact, spectra of secondary electrons play an important role in the induction of DNA breakage. Although photons are always considered as low LET radiation, experiments have demonstrated that not all photons have the same RBE for double-strand break. For instance, the effective LET of the secondary electrons cascade tends to increase as the energy of the primary photon decreases. In the same vein, it has been suggested that X-ray beams are *biologically more effective* than gamma rays from  $^{137}\text{Cs}$  or  $^{60}\text{Co}$  (see e.g., Fig. 2 in [32]).

## 5 Conclusions

1. pBS plasmid DNA fragment-size distributions, following 1.25 MeV gamma irradiation, were measured with AFM resolutions better than 10 nm. These distributions exhibited a discrete-like pattern at all doses, indicating that breakage probabilities by gamma rays are not the same all along the strands.
2. This discrete-like pattern is a modulation of finer and continuous-length distributions of fragments at the AT-rich regions (as in Fig. 4), similar to a randomly broken stick.
3. pBS plasmid fragmentation patterns observed with electron beams are nearly unaffected by quite different dose rates. Their fragment size distributions are *exponential-like decaying functions* as in stochastic phenomena.
4. The similarity between the distributions of AT/TA base pairs and the discrete fragment size lengths obtained with gamma rays is intriguing (Fig. 6), suggesting that gamma radiation shattering of the DNA strands is modulated by the base pair composition.

**Acknowledgements** The authors wish to thank the Institute for Energy and Nuclear Research/IPEN-CNEN in São Paulo, Brazil, for the use of its irradiation facilities. This study was supported by FAPESP and CNPq, Brazilian funding agencies.

## References

1. Schwartz, J.L., Mustafi, R., Beckett, M.A., Czysewski, C.A., Farhangi, E., Grdina, D., Rotmensch, J., Weichselbaum, R.R.: Radiation induced DNA double-strand break frequencies in human squamous cell carcinoma cell lines of different radiation sensitivities. *Int. J. Radiat. Biol.* **59**, 1341–1352 (1991)
2. Blöcher, D., Einspinner, M., Zajackowski, J.: CHEF electrophoresis, a sensitive technique for the determination of DNA double-strand breaks. *Int. J. Radiat. Biol.* **56**, 437–448 (1989)
3. Radford, I.R.: The level of induced DNA double-strand breakage correlates with cell killing after X-irradiation. *Int. J. Radiat. Biol.* **48**, 45–54 (1985)
4. Bradley, M.O., Kohn, K.W.: X-ray induced DNA double-strand break production and repair in mammalian cells as measured by neutral filter elution. *Nucleic Acids Res.* **7**, 793–804 (1979)
5. Pinto, M., Prise, K.M., Michael, B.D.: Quantification of radiation induced DNA double-strand breaks in human fibroblasts by PFGE: testing the applicability of random breakage models. *Int. J. Radiat. Biol.* **78**, 375–388 (2002)
6. Contopoulou, C.R., Cook, V.E., Mortimer, R.K.: Analysis of DNA double-strand breakage and repair using orthogonal field alternation gel electrophoresis. *Yeast* **3**, 71–76 (1987)
7. Cook, V.E., Mortimer, R.K.: A quantitative model of DNA fragments generated by ionizing radiation, and possible experimental applications. *Radiat. Res.* **125**, 102–106 (1991)
8. Cedervall, B., Kallman, P.: Randomly distributed DNA double-strand breaks as measured by pulsed gel electrophoresis: a series of explanatory calculations. *Radiat. Environ. Biophys.* **33**, 9–21 (1994)
9. Cedervall B., Wong, R., Albright, N., Dynlacht, J., Lambin, P., Dewey, W.C.: Methods for the quantification of DNA double-strand breaks determined from the distribution of DNA fragment sizes measured by pulsed-field gel electrophoresis. *Radiat. Res.* **143**, 8–16 (1995), Erratum. *Radiat. Res.* **144**, 122 (1995)

10. Newman, C., Prise, K.M., Folkard, M., Michael, B.D.: DNA double-strand break distributions in X-ray and alpha-particle irradiated V79 cells: evidence for non-random breakage. *Int. J. Radiat. Biol.* **71**, 347–363 (1997)
11. Löbrich, M., Cooper, P.K., Rydberg, B.: Non-random distribution of DNA double-strand breaks induced by particle irradiation. *Int. J. Radiat. Biol.* **70**, 493–503 (1996)
12. Rydberg, B.: Clusters of DNA damage induced by ionizing radiation: formation of short DNA fragments. II. Experimental detection. *Radiat. Res.* **145**, 200–209 (1996)
13. Radmacher, M., Tillman, R.W., Frits, M., Gaub, H.E.: From molecules to cells: imaging soft samples with the atomic force microscope. *Science* **257**, 1900–1905 (1992)
14. Lyubchenko, Y., Shlyakhtenko, L.: Visualization of supercoiled DNA with atomic force microscopy in situ. *Proc. Natl. Acad. Sci. USA* **94**, 496–501 (1997)
15. Hansma, H.G., Laney, D.E., Bezanilla, M., Sinsheimer, R.L., Hansma, P.K.: Applications for atomic force microscopy of DNA. *Biophys. J.* **68**, 1672–1677 (1995)
16. Hansma, H.G.: Surface biology of DNA by atomic force microscopy. *Annu. Rev. Phys. Chem.* **52**, 71–92 (2001)
17. Cary, R.B., Peterson, S.R., Wang, J., Bear, D.G., Bradbury, E.M., Chen, D.J.: DNA looping by Ku and the DNA-dependent protein kinase. *Proc. Natl. Acad. Sci. USA* **94**, 4267–4272 (1997)
18. Smith, G.C.M., Cary, R.B., Lakin, N.D., Hann, B.C., Teo, S.-H., Chen, D.J., Jackson, S.P.: Purification and DNA binding properties of the ataxia-telangiectasia gene product ATM. *Proc. Natl. Acad. Sci. USA* **96**, 11134–11139 (1999)
19. Murakami, M., Hirokawa, H., Hayata, I.: Analysis of radiation damage of DNA by atomic force microscopy in comparison with agarose gel electrophoresis studies. *J. Biochem. Biophys. Methods* **44**, 31–40 (2000)
20. Pang, D.: PhD thesis, The George Washington University, Washington, DC (1997)
21. Pang, D., Vidic, B., Rodgers, J.E., Berman, B.L., Dritschilo, A.: Atomic force microscopy imaging of DNA and DNA repair proteins: applications in radiobiological research. *Radiat. Oncol. Investig.* **5**, 163–169 (1997)
22. Pang, D., Berman, B.L., Chasovskikh, S., Rodgers, J.E., Dritschilo, A.: Investigation of neutron induced damage in DNA by atomic force microscopy: experimental evidence of clustered DNA lesions. *Radiat. Res.* **150**, 612–618 (1998)
23. Pang, D., Rodgers, J.E., Berman, B.L., Chasovskikh, S., Dritschilo, A.: Spatial distribution of radiation induced double-strand breaks in plasmid DNA as resolved by atomic force microscopy. *Radiat. Res.* **164**, 755–765 (2005)
24. Prise, K.M., Newman, H.C., Folkard, M., Michael, B.D.: A study of DNA fragmentation pattern in cells irradiated with charged particles: evidence for non-random distributions. *Phys. Med.* **14**, 20–23 (1998)
25. Wolffe, A.: Chromatin: structure and function, 3rd edn. Academic Press, San Diego (1998)
26. Base pair sequencing of the pBS plasmid could be found at <https://www.lablife.org/g>, <http://www.biovisualtech.com/bvplasmid/pBS-SK-Sfi.htm>, <http://www.biovisualtech.com/sequence/EU573187.txt>
27. Lodish, H., et al.: *Molecular Cell Biology*, 4th edn, p. 107. Freeman & Co., New York (1999). Figs. 4–9
28. Heller, A.: Spiers memorial lecture. On the hypothesis of cathodic protection of genes. *Faraday Discuss.* **116**, 1–13 (2000)
29. Sanche, L.: Nanoscopic aspects of radiobiological damage: fragmentation induced by secondary low-energy electrons. *Mass Spectrom. Rev.* **21**, 349–369 (2002)
30. Huels M.A., Boudaïffa B., Cloutier P., Hunting D., Sanche L.: Single, double, and multiple double-strand breaks induced in DNA by 3–100 eV electrons. *J. Am. Chem. Soc.* **125**, 4467–4477 (2003)
31. Denifl, S., Sulzer, P., Huber, D., Zappa, F., Probst, M., Märk, T.D., Scheier, P., Injan, N., Limtrakul, J., Abouaf, R., Dunet, H.: Influence of functional groups on the site-selective dissociation of adenine upon low-energy electron attachment. *Angew. Chem. Int. Ed.* **46**, 5238–5241 (2007)
32. Hsiao, Y., Stewart, R.D.: Monte Carlo simulation of DNA damage induction by X-rays and selected isotopes. *Phys. Med. Biol.* **53**, 233–244 (2008)